Clemson University
College of Engineering and Science
Control and Robotics (CRB) Technical Report

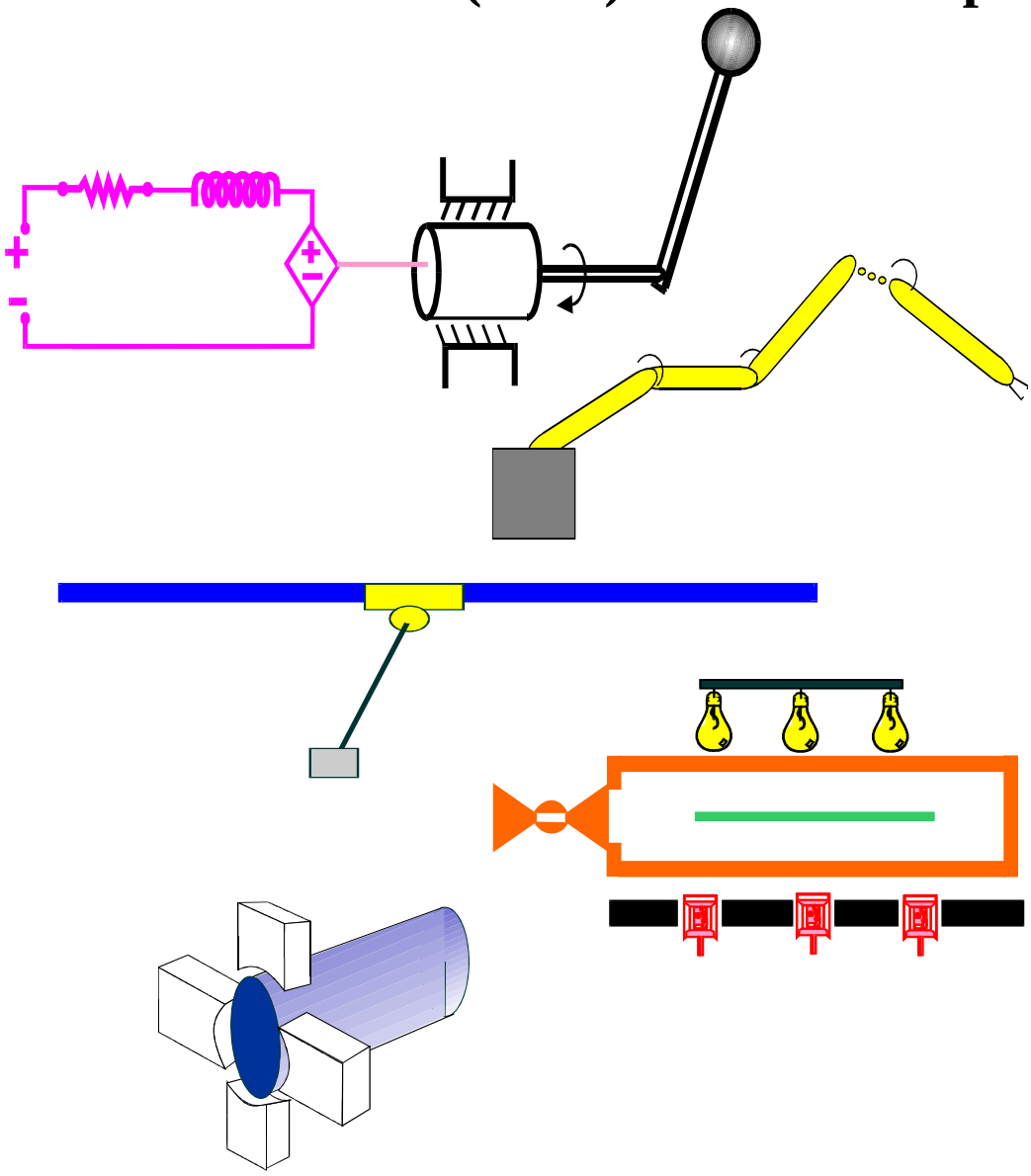

Number: CU/CRB/10/2/06/#1

Title: Adaptive and Robust Control for Thermal Management Systems

Authors: M. Salah, T. Mitchel, J. Wagner, and D. Dawson

Report Documentation Page

Form Approved
OMB No. 0704-0188

1. REPORT DATE	2. REPORT TYPE	3. DATES COVERED
2006		**00-00-2006 to 00-00-2006**

4. TITLE AND SUBTITLE	5a. CONTRACT NUMBER
Adaptive and Robust Control for Thermal Management Systems	5b. GRANT NUMBER
	5c. PROGRAM ELEMENT NUMBER
6. AUTHOR(S)	5d. PROJECT NUMBER
	5e. TASK NUMBER
	5f. WORK UNIT NUMBER
7. PERFORMING ORGANIZATION NAME(S) AND ADDRESS(ES) **Clemson University,Automotice Research Laboratory,Departments of Mechanical and Electrical Engineering,Clemson,SC,29634-0921**	8. PERFORMING ORGANIZATION REPORT NUMBER
9. SPONSORING/MONITORING AGENCY NAME(S) AND ADDRESS(ES)	10. SPONSOR/MONITOR'S ACRONYM(S)
	11. SPONSOR/MONITOR'S REPORT NUMBER(S)

12. DISTRIBUTION/AVAILABILITY STATEMENT
Approved for public release; distribution unlimited

13. SUPPLEMENTARY NOTES
The original document contains color images.

14. ABSTRACT

15. SUBJECT TERMS

16. SECURITY CLASSIFICATION OF:			17. LIMITATION OF ABSTRACT	18. NUMBER OF PAGES	19a. NAME OF RESPONSIBLE PERSON
a. REPORT	b. ABSTRACT	c. THIS PAGE			
unclassified	**unclassified**	**unclassified**		**15**	

Adaptive and Robust Control for Thermal Management Systems

M. H. Salah[†], T. H. Mitchell[‡], Dr. J. R. Wagner[‡] P.E., and Dr. D. M. Dawson[†] P.E.

Automotive Research Laboratory
Departments of Mechanical[‡] and Electrical[†] Engineering
Clemson University, Clemson, SC 29634-0921
(864) 656-7376, jwagner@clemson.edu

ABSTRACT

Advanced thermal management systems for internal combustion engines can improve coolant temperature regulation and servomotor power consumption by better regulating the combustion process with multiple electro-mechanical components. The traditional thermostat valve, coolant pump and clutch-driven radiator fan are upgraded with servomotor actuators. When the system components function harmoniously, desired thermal conditions can be accomplished in a power efficient manner. In this paper, a comprehensive control architecture is proposed for transient temperature tracking. An experimental system has been fabricated and assembled which features a variable position smart thermostat valve, variable speed electric water pump, variable speed electric radiator fan, engine block, and various sensors. In the configured system, the steam-based heat exchanger emulates the heat generated by the engine's combustion process. Representative numerical and experimental results are discussed to demonstrate the functionality of the thermal management system in tracking prescribed temperature profiles.

1. INTRODUCTION

Internal combustion engine active thermal management systems offer enhanced coolant temperature tracking control during transient and steady-state operation. Although the conventional automotive cooling system has proven satisfactory for many decades, servo-motor controlled cooling components have the potential to reduce the fuel consumption, parasitic losses, and tailpipe emissions (Brace *et al.*, 2001). Advanced automotive cooling systems replace the conventional wax thermostat valve with a controllable position smart valve, and replace the mechanical water pump and radiator fan with electric and/or hydraulic driven actuators (Choukroun and Chanfreau, 2001). This replacement decouples the water pump and radiator fan from the engine crankshaft, and this solves the problem of having over/under cooling, due to the mechanical coupling, and parasitic losses associated with running mechanical components at high rotational speeds that increase exponentially (Chalgren and Barron, 2003). An assessment of thermal management strategies for large on-highway trucks and high-efficiency vehicles were described by Wambsganss (1999). Chanfreau *et al.* (2001) studied the benefits of engine cooling with fuel economy and emissions over the FTP drive cycle on a dual voltage 42V-12V minivan.

Cho *et al.* (2004) investigated a controllable electric water pump in a class-3 medium duty diesel engine trucks. It was shown that the radiator size can be reduced by replacing the mechanical pump with an electrical one. Chalgren and Allen (2005) and Chalgren and Traczyk (2005) improved the temperature control, while decreasing parasitic losses, by replacing the conventional cooling system of a light duty diesel truck with an electric cooling system.

To create an efficient automotive thermal management system, the vehicle's cooling system behavior and transient response must be analyzed. Wagner *et al.* (2001, 2002, 2003) pursued a lumped parameter modeling approach and presented multi-node thermal models which estimate internal engine temperature. Eberth *et al.* (2004) presented a mathematical model to analytically predict the dynamic behavior of a 4.6L spark ignition engine. To accompany the mathematical models, analytical/empirical descriptions were developed to describe the smart cooling system components. Henry *et al.* (2001) developed a simulation model of powertrain cooling systems for ground vehicles. The model was validated against test results which featured basic system components (*e.g.*, radiator, water pump, surge (return) tank, hoses and pipes, and engine thermal load).

A multiple node lumped parameter-based thermal network with a suite of mathematical models, describing controllable electromechanical actuators, was introduced by Setlur *et al.* (2005). The proposed simplified cooling system used immersion DC heaters to emulate the engine's combustion process and control components, with nonlinear control algorithms, to regulate the temperature. In their experiments, the water pump and radiator fan were

set to run at constant speeds, while the smart valve was controlled to trade coolant temperature set point. Cipollone and Villante (2004) tested three cooling control schemes (*e.g.*, closed-loop, model-based, and mixed) and compared them against a traditional "thermostat-based" controller. Page *et al.* (2005) conducted experimental tests on a medium-sized tactical vehicle that was equipped with an intelligent thermal management system. The authors investigated improvements in the engine's peak fuel consumption and thermal operating conditions. Finally, Redfield *et al.* (2006) operated a class 8 tractor at highway speeds to study potential energy saving and demonstrate engine cooling to with ±3ºC of set point value.

In this paper, a nonlinear control strategy is presented to actively regulate the coolant temperature in internal combustion engines. An advanced thermal management system was implemented on a laboratory test bench that features a smart thermostat valve, variable speed electric water pump and fan, radiator, engine block, and a steam-based heat exchanger to emulate the combustion heating process. The proposed control strategies have been verified by simulation and validated by experimental testing. In Section 2, the cooling system model is presented to describe the thermal system dynamics. Nonlinear tracking control strategies are introduced in Section 3. Section 4 presents the experimental steam test bench while Section 5 introduces numerical results. Experimental results are introduced in Section 6. The conclusion is contained in Section 7. The Appendices present a Lyapunov-based stability analysis, which is needed for the controller's design, as well as the Nomenclature List.

2. COOLING SYSTEM MODEL

A reduced order two-node lumped parameter thermal model is used, as shown in Fig 1, to represent the transient response of the advanced cooling system. The system components are a 4.6L engine block, a radiator block with a variable speed electric fan, a variable position three-way smart valve, a variable speed electric water pump, and a steam-based heat exchanger to emulate the heat generated by the combustion process.

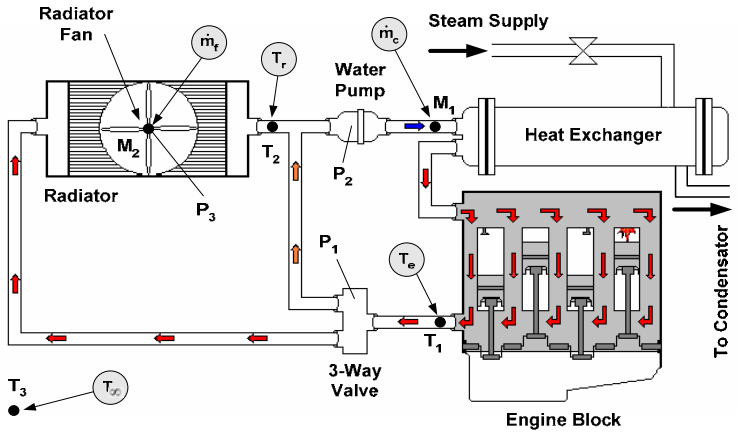

Fig 1 *Advanced cooling system which features a smart valve, variable speed pump, variable speed fan, engine block, radiator, and sensors (temperature, mass flow rate, and power)*

This simplified model is used to reduce the computational burden for in-vehicle implementation. The dynamics of the engine and radiator blocks at the selected nodes, as shown in Fig 1, can be described by the following differential equations

$$C_e \dot{T}_e = Q_{in} - C_{pc} \dot{m}_r \left(T_e - T_r \right) \tag{1}$$

$$C_r \dot{T}_r = C_{pc} \dot{m}_r \left(T_e - T_r \right) - Q_o + \varepsilon C_{pa} \dot{m}_f \left(T_e - T_\infty \right). \tag{2}$$

Because a three-way valve is used in the system, the variable $\dot{m}_r(t)$ is defined as $\dot{m}_r = H\dot{m}_c$, where the variable $H(t)$ satisfies the condition $0 \le H(t) \le 1$. Note that $H(t) = 1(0)$ corresponds to a fully closed (open) valve position and coolant flow through the bypass (radiator) loop. To facilitate the controller design process, four assumptions are imposed.

Assumption 1: The system parameters; C_{pc}, C_{pa}, C_e, C_r and ε are assumed to be constants and fully known.

***Assumption 2*:** It is assumed that the engine block and radiator block temperatures satisfy $T_e(t) - T_r(t) \geq \varepsilon_2, \forall t \geq 0$ where $\varepsilon_2 \in \Re^+$ is a constant. Further we assume that $T_e(0) \geq T_r(0)$ to facilitate the boundedness of signal argument.

***Assumption 3*:** It is assumed that the surrounding ambient temperature $T_\infty(t)$ is constant and satisfies $T_r(t) - T_\infty(t) \geq \varepsilon_1, \forall t \geq 0$ where $\varepsilon_1 \in \Re^+$ is a constant.

Assumption 4: From the problem physics, the signals $Q_{in}(t)$ and $Q_o(t)$ always remain positive in (1), and (2) (i.e. $Q_{in}(t), Q_o(t) \geq 0$).

3. THERMAL CONTROL SYSTEM DESIGNS

In this paper, two Lyapunov-based nonlinear control algorithms are presented to maintain a desired thermal condition for the engine block. The objective of the proposed control strategies is to get a precise engine temperature tracking while compensating for the system uncertainties (e.g. combustion process heat input and external ram air disturbance) by harmoniously controlling the system actuators.

The control objective of the nonlinear control strategies is to ensure that the actual temperatures of the engine block $T_e(t)$ and the radiator block $T_r(t)$ track the desired trajectories $T_{ed}(t)$ and $T_{rd}(t)$, respectively, in the following sense

$$T_e(t) \to T_{ed}(t) \quad \text{as } t \to \infty, \qquad T_r(t) \to T_{rd}(t) \quad \text{as } t \to \infty \tag{3}$$

while compensating for the system uncertainties $Q_{in}(t)$ and $Q_o(t)$.

Remark 1: It is assumed that the desired engine and radiator temperature profiles are selected such that they are always bounded and their first three time derivatives remain bounded at all times (*i.e.*, $T_{ed}(t), \dot{T}_{ed}(t), \ddot{T}_{ed}(t), \dddot{T}_{ed}(t), T_{rd}(t), \dot{T}_{rd}(t), \ddot{T}_{rd}(t), \dddot{T}_{rd}(t) \in L_\infty$. Further more, $T_{ed}(t) >> T_{rd}(t) >> T_\infty$ at all times.

3.1 Adaptive Control Strategy

To facilitate the controller's development and quantify the temperature tracking control objective, the following signals are defined

$$e \triangleq T_{ed} - T_e, \qquad \eta \triangleq T_{rd} - T_r. \tag{4}$$

Assumption 5: It is assumed that the signals $Q_{in}(t)$ and $Q_o(t)$ are constants at all time.

3.1.1 Closed-Loop Error System Development and Controller Formulation

The open-loop error system can be analyzed by taking the first time derivative of both expressions in (4) and then multiplying both sides of the resulting equations by C_e and C_r for the engine and radiator dynamics, respectively. Thus, the system dynamics described in (1) and (2) can be substituted and then reformatted to realize

$$C_e\dot{e} = C_e\dot{T}_{ed} - \theta_e + u_e, \qquad C_r\dot{\eta} = C_r\dot{T}_{rd} + \theta_r - u_r \tag{5}$$

where $\theta_e(t) = Q_{in}(t)$, $\theta_r(t) = Q_o(t)$, $u_e(t) \triangleq C_{pc}\dot{m}_r(T_e - T_r)$, and $u_r(t) \triangleq C_{pc}\dot{m}_r(T_e - T_r) - \varepsilon C_{pa}\dot{m}_f(T_e - T_\infty)$.

Remark 2: *The control inputs $\dot{m}_r(t)$ and $\dot{m}_f(t)$ are uni-polar. Hence, commutation strategies are designed to implement the bi-polar inputs $u_e(t)$ and $u_r(t)$ as*

$$\dot{m}_r \triangleq \frac{u_e\left[1+\text{sgn}(u_e)\right]}{2C_{pc}(T_e - T_r)}, \qquad \dot{m}_f \triangleq \frac{F\left[1+\text{sgn}(F)\right]}{2\varepsilon C_{pa}(T_e - T_\infty)} \tag{6}$$

where $F(t) \triangleq C_{pc}\dot{m}_r(T_e - T_r) - u_r$. The control input, $\dot{m}_f(t)$ is obtained from (6) after $\dot{m}_r(t)$ is computed. From these definitions, it is clear that if $u_e(t), u_r(t) \in L_\infty \forall t \geq 0$, then $\dot{m}_r(t), \dot{m}_f(t) \in L_\infty \forall t \geq 0$. From the calculation of

the radiator mass flow rate $\dot{m}_r(t)$ and using a three-way valve in the system, the water pump speed can be determined for a given valve position or the valve position can be determined for a given water pump speed.

To satisfy the control objectives stated earlier, continuous control laws $u_e(t)$ and $u_r(t)$ can be designed as follows

$$u_e = \hat{\theta}_e - C_e\dot{T}_{ed} - K_e e\,, \qquad u_r = \hat{\theta}_r + C_r\dot{T}_{rd} + K_r\eta \tag{7}$$

where the estimates $\hat{\theta}_e(t)$ and $\hat{\theta}_r(t)$ are to compensate for the system constants uncertainties $Q_{in}(t)$ and $Q_o(t)$, and designed as follows

$$\hat{\theta}_e = -\alpha_e\int_{t_o}^{t} e(\tau)\,d\tau\,, \qquad \hat{\theta}_r = \alpha_r\int_{t_o}^{t}\eta(\tau)\,d\tau \tag{8}$$

3.1.2 Stability Analysis

Theorem 1: The controller given in (7) ensures asymptotic engine and radiator temperatures tracking (i.e. $e(t),\eta(t)\to 0$ as $t\to\infty$) and all closed-loop signals are bounded.

Proof: See Appendix A for the complete Lyapunov-based stability analysis.

3.2 Robust Control Strategy

To facilitate the controllers' development and quantify the temperature tracking control objective, a filtered tracking error is defined as follows

$$s_e \triangleq \dot{e} + \alpha_e e\,, \qquad s_r \triangleq \dot{\eta} + \alpha_r\eta \tag{9}$$

where $e(t)$ and $\eta(t)$ were defined in (4).

Assumption 6: It is assumed that the signals $Q_{in}(t)$ and $Q_o(t)$ vary with time and their first two time derivatives remain bounded at all time, such that $Q_{in}(t),\dot{Q}_{in}(t),\ddot{Q}_{in}(t),Q_o(t),\dot{Q}_o(t),\ddot{Q}_o(t)\in L_\infty$.

3.2.1 Closed-Loop Error System Development and Controller Formulation

The open-loop error system can be analyzed by taking the first time derivative of both expressions in (9) and then multiplying both sides of the resulting equations by C_e and C_r for the engine and radiator dynamics, respectively. Thus, the system dynamics described in (1) and (2) can be substituted and then reformatted to realize

$$C_e\dot{s}_e = C_e\ddot{T}_{ed} - \dot{Q}_{in} + \dot{u}_e + C_e\alpha_e\dot{e}\,, \qquad C_r\dot{s}_r = C_r\ddot{T}_{rd} + \dot{Q}_o - \dot{u}_r + C_r\alpha_r\dot{\eta} \tag{10}$$

where (4) and it is first time derivative were utilized provided the signals $u_e(t)$ and $u_r(t)$ are defined as $u_e(t)\triangleq C_{pc}\dot{m}_r(T_e - T_r)$ and $u_r(t)\triangleq C_{pc}\dot{m}_r(T_e - T_r) - \varepsilon C_{pa}\dot{m}_f(T_r - T_\infty)$.

Remark 3: *The control inputs $\dot{m}_r(t)$ and $\dot{m}_f(t)$ are uni-polar. Hence, the commutation strategies, designed in (6), are used to implement the bi-polar inputs $u_e(t)$ and $u_r(t)$.*

To facilitate the subsequent analysis, the expressions in (10) are rewritten as follows

$$C_e\dot{s}_e = \tilde{N}_e + N_{ed} + \dot{u}_e - e\,, \qquad C_r\dot{s}_r = \tilde{N}_r + N_{rd} - \dot{u}_r - \eta \tag{11}$$

where the auxiliary signals $\tilde{N}_e(\dot{T}_e, T_e, t)$ and $\tilde{N}_r(\dot{T}_r, T_r, t)$ are defined as follows

$$\tilde{N}_e = N_e - N_{ed}\,, \qquad \tilde{N}_r = N_r - N_{rd} \tag{12}$$

where $N_e\left(\dot{T}_e, T_e, t\right)$ and $N_r\left(\dot{T}_r, T_r, t\right)$ are defined as follows

$$N_e \triangleq C_e \ddot{T}_{ed} - \dot{Q}_{in} + C_e \alpha_e \dot{e} + e\,, \qquad N_r \triangleq C_r \ddot{T}_{rd} + \dot{Q}_o + C_r \alpha_r \dot{\eta} + \eta \tag{13}$$

and both $N_{ed}(t)$ and $N_{rd}(t)$ are defined as follows

$$N_{ed} \equiv N_e\Big|_{T_e = T_{ed}, \dot{T}_e = \dot{T}_{ed}} = C_e \ddot{T}_{ed} - \dot{Q}_{in}\,, \qquad N_{rd} \equiv N_r\Big|_{T_r = T_{rd}, \dot{T}_r = \dot{T}_{rd}} = C_r \ddot{T}_{rd} + \dot{Q}_o\,. \tag{14}$$

Based on (12) through (14), the control laws introduced in (11) are designed as follows

$$u_e = -\left(K_e + \alpha_e\right)\left[e - e_o\right] - \int_{t_o}^{t} \left[\alpha_e \left(K_e + \alpha_e\right) e(\tau) + \rho_e \operatorname{sgn}(e(\tau))\right] d\tau \tag{15}$$

$$u_r = \left(K_r + \alpha_r\right)\left[\eta - \eta_o\right] + \int_{t_o}^{t} \left[\alpha_r \left(K_r + \alpha_r\right) \eta(\tau) + \rho_r \operatorname{sgn}(\eta(\tau))\right] d\tau \tag{16}$$

where e_o, η_o are $e(t), \eta(t)$, respectively, computed at the initial time t_o. The terms e_o and η_o in (15) and (16), respectively, are included so that $u_e(t_o)$ and $u_e(t_o)$ equal to zero, where the "sgn" terms compensate for the unknown quantities in (13). The time derivatives of (15) and (16) are given by the following expressions

$$\dot{u}_e = -\left(K_e + \alpha_e\right) s_e - \rho_e \operatorname{sgn}(e)\,, \qquad \dot{u}_r = \left(K_r + \alpha_r\right) s_r + \rho_r \operatorname{sgn}(\eta)\,. \tag{17}$$

After substituting (17) into (11), the closed-loop error system can be obtained as follows

$$C_e \dot{s}_e = \tilde{N}_e + N_{ed} - \left(K_e + \alpha_e\right) s_e - \rho_e \operatorname{sgn}(e) - e \tag{18}$$

$$C_r \dot{s}_r = \tilde{N}_r + N_{rd} - \left(K_r + \alpha_r\right) s_r - \rho_r \operatorname{sgn}(\eta) - \eta\,. \tag{19}$$

Remark 4**:** *Based on Remark 1, Assumption 6, and the expressions in (14),* $\left|N_{ed}(t)\right|, \left|\dot{N}_{ed}(t)\right|, \left|N_{rd}(t)\right|$ *and* $\left|\dot{N}_{rd}(t)\right|$ *can be upper bounded by known positive constants as follows*

$$\left|N_{ed}\right| \le \zeta_{e1}\,, \qquad \left|\dot{N}_{ed}\right| \le \zeta_{e2}\,, \qquad \left|N_{rd}\right| \le \zeta_{r1}\,, \qquad \left|\dot{N}_{rd}\right| \le \zeta_{r2}\,. \tag{20}$$

3.2.2 Stability Analysis

Theorem 2: The controller given in (15) and (16) ensures asymptotic engine and radiator temperatures tracking (i.e. $e(t), s_e(t), \eta(t), s_r(t) \to 0$ as $t \to \infty$) and all closed-loop signals are bounded provided the control gains ρ_e and ρ_r are selected to satisfy the following sufficient conditions

$$\rho_e > \zeta_{e1} + \frac{1}{\alpha_e}\zeta_{e2}\,, \qquad \rho_r > \zeta_{r1} + \frac{1}{\alpha_r}\zeta_{r2} \tag{21}$$

where $\zeta_{e1}, \zeta_{e2}, \zeta_{r1}$ and ζ_{r2} are given in (20), and K_e and K_r are selected sufficiently large.

Proof: See Appendix B for the complete Lyapunov-based stability analysis.

4. STEAM TEST BENCH

An experimental test bench (refer to Figure 2) has been fabricated to demonstrate the proposed advanced thermal management system controller design. The assembled test bench offers a flexible, rapid, repeatable, and safe testing environment. Clemson University facilities generated steam is utilized to rapidly heat the coolant circulating within the cooling system via a two-pass shell and tube heat exchanger. The heated coolant is then routed through a 6.0L diesel engine block to emulate the combustion process heat. From the engine block, the coolant flows to a three-way smart valve and then either through the bypass or radiator to the water pump to close the loop. The thermal response

of the engine block to the adjustable, externally applied heat source emulates the heat transfer process between the combustion gases, cylinder wall, and water jacket in an actual operating engine. As shown in Figure 1, the system sensors include three type-J thermocouples (e.g., T_1 = engine temperature, T_2 = radiator temperature, and T_3 = ambient temperature), two mass flow meters (e.g., M_1 = coolant mass flow meter, and M_2 = air mass flow meter), and electric voltage and current measurements (e.g., P_1 = valve power consumed, P_2 = pump power consumed, and P_3 = fan power consumed).

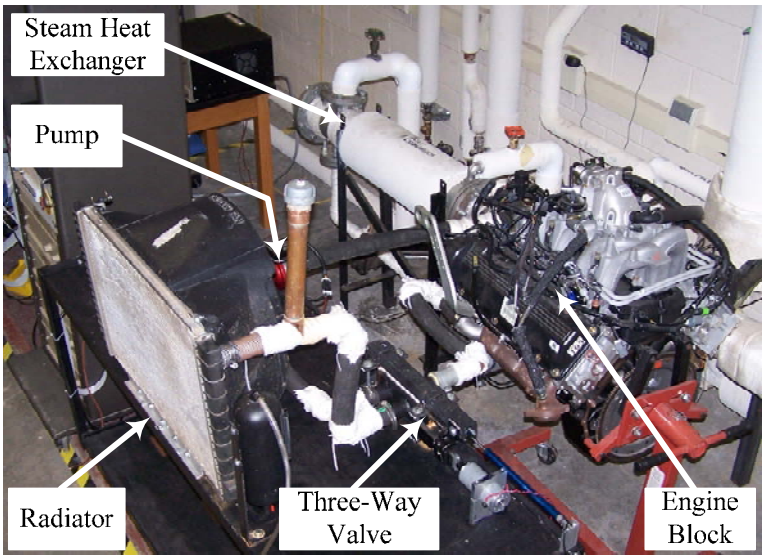

Fig 2 *Experimental thermal test bench that features a 6.0L diesel engine block, three-way smart valve, electric water pump, electric radiator fan, radiator, and steam-based heat exchanger*

The steam bench can provide up to 55 kW of energy. High pressure saturated steam (412 kPa) is routed from the campus facilities plant to the steam test bench, where a pressure regulator reduces the steam pressure to 172 kPa before it enters the low pressure filter. The low pressure saturated steam is then routed to the double pass steam heat exchanger to heat the system's coolant. The amount of energy transferred to the system is controlled by the main valve mounted on the heat exchanger. The mass flow rate of condensate is proportional to the energy transfer to the circulating coolant. Condensed steam may be collected and measured to calculate the rate of energy transfer. From steam tables, the enthalpy of condensation can be acquired. To facilitate the analysis, pure saturated steam and condensate at approximately T=100ºC determines the enthalpy of condensation. Baseline testing was performed to determine the average energy transferred to the coolant at various steam control valve positions. The coolant temperatures were initialized at T_e = 67ºC before measuring the condensate. Each test was executed for different time periods.

5. SIMULATION RESULTS

5.1 Adaptive Control

Test 1: Constant Heat Input and External Disturbance

A numerical simulation for the adaptive control strategy, introduced in Section 3.1, has been performed on the system dynamics described in (1) and (2) to demonstrate the performance of the proposed controller given in (7) and (8). The simulated thermal system's parameters were set to the following: $C_e = C_r = 63250$ [J/ºK], $C_{pc} = 4186$ [J/kg.ºK], $C_{pa} = 1000$ [J/kg.ºK], $\varepsilon = 0.6$, $T_\infty(t) = 300$ [ºK], $\dot{m}_c(t) = 0.8214$ [kg/sec], $Q_{in}(t) = 30$ [kW] and $Q_o(t) = 7$ [kW]. The initial simulation conditions were set to be as follows: $T_e(0) = 360$ [ºK] and $T_r(0) = 347$ [ºK]. The desired temperatures were selected to be $T_{ed}(t) = 350 + \sin(0.05t)$ [ºK] and $T_{rd}(t) = 340$ [ºK]. The controller gains were set to be as follows: $K_e = 1000$, $K_r = 10$ and $\alpha_e = \alpha_r = 0.1$. The engine and radiator temperatures response is presented in Fig 3, while the normalized valve position and fan response is shown in Fig 4.

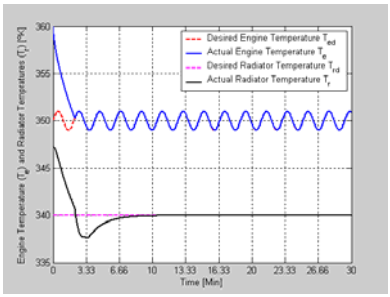

Fig 3 *Engine & radiator temperatures response*

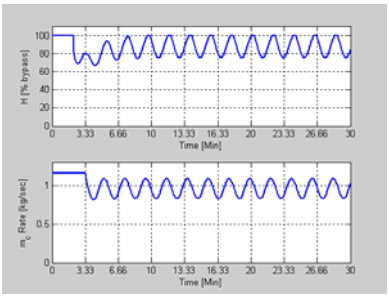

Fig 4 *Normalized valve position & fan response*

Test 2: Variable Heat Input and External Disturbance

A numerical simulation for the adaptive control strategy, introduced in Section 3.1, has been performed on the system dynamics described in (1) and (2) to demonstrate the performance of the proposed controller given in (7) and (8). The simulated thermal system's parameters were set as in Test 1 except for $Q_{in}(t)$ and $Q_o(t)$, where $Q_o(t) = 10 + 3\sin(0.05t)$ [kW] and $Q_{in}(t)$ as shown in Fig 5. The heat input is designed as shown in Fig 5 to verify the reliability of the control design and performance under different levels of disturbance. The initial simulation conditions and desired temperatures were also selected as in Test 1. The controller gains K_r and α_r were reset to be as follows: $K_r = 500$ and $\alpha_r = 0.01$. The engine and radiator temperatures response is presented in Fig 6, while the normalized valve position and fan response is shown in Fig 7.

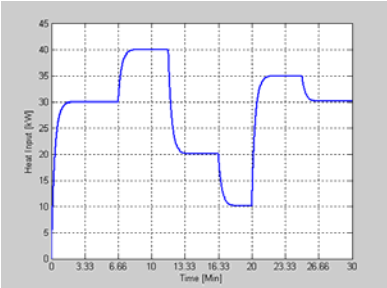

Fig 5 *Heat Input*

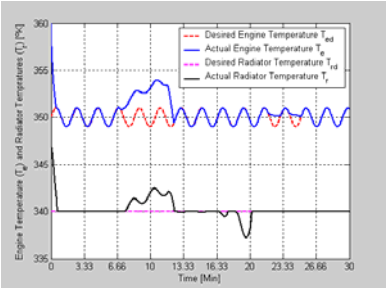

Fig 6 *Engine and radiator temperatures response*

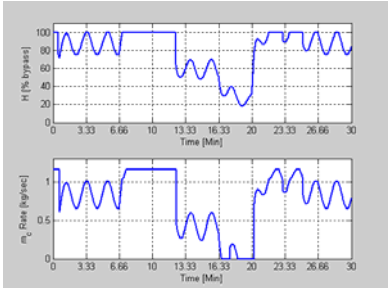

Fig 7 *Normalized valve position and fan response*

When the heat input is set to be high (40 or 35 [kW]), the valve routs the coolant only through the radiator loop and the fan runs at its maximum speed as shown in Fig 7. The valve and fan efforts, in fact, are not enough to cool down the engine temperature as shown in Fig 8 because of the extra heat added to the system that can not be handled.

5.2 Robust Control

Test 3: Constant Heat Input and External Disturbance

A numerical simulation for the robust control strategy, introduced in Section 3.2, has been performed on the system dynamics described in (1) and (2) to demonstrate the performance of the proposed controller given in (15) and (16). The simulated thermal system's parameters, initial simulation conditions, and desired temperatures were set as in Test 1. The controller gains were set to be as follows: $K_e = 1000$, $K_r = 100$, $\alpha_e = \alpha_r = 0.1$ and $\rho_e = \rho_r = 0.5$. The engine and radiator temperatures response is presented in Fig 8, while the normalized valve position and fan response is shown in Fig 9.

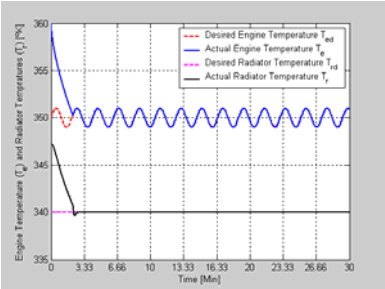

Fig 8 *Engine & radiator temperatures response*

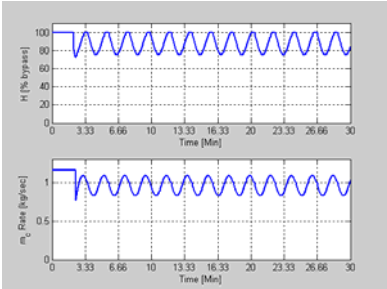

Fig 9 *Normalized valve position & fan response*

Test 4: Variable Heat Input and External Disturbance

A numerical simulation for the robust control strategy, introduced in Section 3.2, has been performed on the system dynamics described in (1) and (2) to demonstrate the performance of the proposed controller given in (15) and (16). The simulated thermal system's parameters, initial simulation conditions, and desired temperatures were set as in Test 1. The controller gains were reset to be as follows: $K_e = 1000$, $K_r = 500$, $\alpha_e = 5$, $\alpha_r = 0.1$ and $\rho_e = \rho_r = 0.01$. The engine and radiator temperatures response is presented in Fig 10, while the normalized valve position and fan response is shown in Fig 11. From Fig 10, it is clear that the robust control can not handle the extra heat added to the system as in the adaptive control.

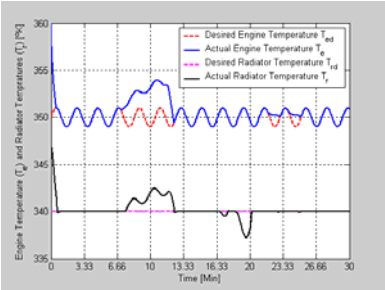

Fig 10 *Engine and radiator temperatures response*

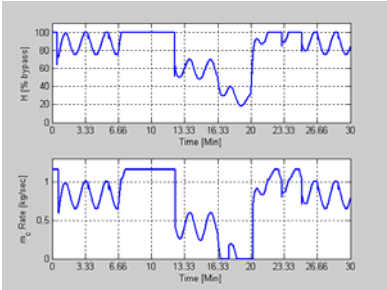

Fig 11 *Normalized valve position and fan response*

Table 1 shows a summery for the simulation results. From Table 1, it is clear that the steady state of the engine temperature tracking error is about the same for all the proposed control strategies. It is also clear that the performance of both control strategies are quite the same in terms of power measure and handling the heat variations. The power measure is found as follows

$$P_{sys} = \int_{t_o}^{t} \left[\dot{m}_c^2(\tau) + \dot{m}_f^2(\tau) \right] d\tau \tag{22}$$

where the power consumed by the system actuators mainly depends on how much coolant and air mass flow rates are needed. On the other hand, the power consumed by the valve is considered very small and neglected.

Test #	Description	Steady State Error [°K]	Power Measure
1	Adaptive control (Q_{in} / Q_o are constants)	[-0.03, 0]	2952
2	Adaptive control (Q_{in} / Q_o are variables)	[-0.03, 0]	2529
3	Robust control (Q_{in} / Q_o are constants)	[-0.03, 0.015]	2939
4	Robust control (Q_{in} / Q_o are variables)	[-0.03, 0.005]	2528

Table 1 Simulation results summery

6. EXPERIMENTAL RESULTS

…….

7. CONCLUSION

Advanced automotive thermal management system can have a positive impact on gasoline and diesel engine cooling systems. In this paper, a suit of servo-motor based-cooling system components have been assembled and controlled using a Lyapunov-based nonlinear control technique. The control algorithm has been investigated using both simulation and experimental tests. Two detailed and two supplemental controllers were applied to regulate the engine temperature. In each instance, the controllers successfully maintained the engine block to setpoint temperatures with small error percentages. It has also been shown that the power consumed by the system actuators can be reduced. Overall, the findings demonstrated that setpoint temperatures can be maintained satisfactory while minimizing power consumption which ultimately impacts fuel economy.

ACKNOWLEDGEMENTS
The authors would like to thank the U.S. Army Tank-Automotive and Armaments Command (TACOM), and the Automotive Research Center (ARC) at the University of Michigan and Clemson University for funding this project.

REFERENCES

Brace, C., Burnham-Slipper, H., Wijetunge, R., Vaughan, N., Wright, K., and Blight, D., "Integrated Cooling Systems for Passenger Vehicles," SAE technical paper No. 2001-01-1248, 2001.

Chalgren, Jr, R., and Allen, D., "Light Duty Diesel Advanced Thermal Management," SAE technical paper No. 2005-01-2020, 2005.

Chalgren, Jr, R., and Barron, Jr, L., "Development and Verification of a Heavy Duty 42/14V Electric Powertrain Cooling System," SAE technical paper No. 2003-01-3416, 2003.

Chalgren, Jr, R., and Traczyk, T., "Advanced Secondary Cooling Systems for Light Trucks," SAE technical paper No. 2005-01-1380, 2005.

Chanfreau, M., Joseph, A., Butler, D., and Swiatek, R., "Advanced Engine Cooling Thermal Management System on a Dual Voltage 42V-14V Minivan," SAE technical paper No. 2001-01-1742, 2001.

Cho, H., Jung, D., Filipi, Z., and Assanis, D., "Application of Controllable Electric Coolant Pump for Fuel Economy and Cooling Performance Improvement," proceedings of the ASME IMECE, Advanced Energy Systems Division, vol. 44, pp. 43-50, Anaheim, CA, November 2004.

Choukroun, A., and Chanfreau, M., "Automatic Control of Electric Actuators for an Optimized Engine Cooling Thermal Management," SAE technical paper No. 2001-01-1758, 2001.

Cipollone, R., and Villante, C., "Vehicle Thermal Management: A Model-Based Approach," proceedings of the ASME Internal Combustion Engine Division, pp. 85-95, Long Beach, CA, October 2004.

Eberth, J., Wagner, J., Afshar, B., and Foster, R., "Modeling and Validation of Automotive "Smart" Thermal Management System Architecture," SAE technical paper No. 2004-01-0048, 2004.

Henry, R., Koo, J., and Richter, C., "Model Development, Simulation and Validation, of Power Train Cooling System for a Truck Application," SAE paper No. 2001-01-1731, 2001.

Khalil, H., "Nonlinear Systems," 3rd Edition, Upper Saddle River, NJ: Prentice-Hall, Inc., 2002.

Page, R., Hnatczuk, W., and Kozierowski, J., "Thermal Management for the 21st Century – Improved Thermal Control & Fuel Economy in an Army Medium Tactical Vehicle," SAE paper No. 2005-01-2068, 2005.

Redfield, J., Surampudi, B., Ray, G., Montemayor, A., Mckee, H., Edwards, T., and Lasecki, M., "Accessory Electrification in Class 8 Tractors," SAE paper No. 2006-01-0215, 2006.

Setlur, P., Wagner, J., Dawson, D., and Marotta, E., "An Advanced Engine Thermal Management System: Nonlinear Control and Test", *IEEE/ASME Transactions on Mechatronics*, vol. 10, no. 2, pp. 210-220, April 2005.
Wagner, J., Marotta, E., and Paradis, I., "Thermal Modeling of Engine Components for Temperature Prediction and Fluid Flow Regulation", SAE technical paper No. 2001-01-1014, 2001.

Wagner, J., Ghone, M., Dawson, D., and Marotta, E., "Coolant Flow Control Strategies for Automotive Thermal Management Systems," SAE technical paper No. 2002-01-0713, 2002.

Wagner, J., Srinivasan, V., and Dawson, D., "Smart Thermostat and Coolant Pump Control for Engine Thermal Management Systems," SAE technical paper No. 2003-01-0272, 2003.

Wambsganss, M., "Thermal Management Concepts for Higher-Efficiency Heavy Vehicle," SAE technical paper No. 1999-01-2240, 1999.

APPENDIX A
Proof of Theorem 1

Let $V(z,t) \in \Re$ denote the following non-negative function

$$V \triangleq \frac{1}{2}C_e e^2 + \frac{1}{2\alpha_e}\tilde{\theta}_e^{\,2} + \frac{1}{2}C_r \eta^2 + \frac{1}{2\alpha_r}\tilde{\theta}_r^{\,2} \tag{22}$$

where $z(t) \in \Re^2$ is defined as follows

$$z \triangleq \begin{bmatrix} e & \eta \end{bmatrix}^T. \tag{23}$$

Note that (22) is bounded as follows

$$\lambda_1 \|z(t)\|^2 \le V(z,t) \le \lambda_2 \|z(t)\|^2 \tag{24}$$

where λ_1, λ_2 are positive constants. After taking the time derivative of (22), the following expression can be obtained

$$\dot{V} = e\left(\tilde{\theta}_e - K_e e\right) + \frac{1}{\alpha_e}\tilde{\theta}_e\dot{\tilde{\theta}}_e + \eta\left(-\tilde{\theta}_r - K_r\eta\right) + \frac{1}{\alpha_r}\tilde{\theta}_r\dot{\tilde{\theta}}_r \tag{25}$$

where (5) and (7) were utilized, and the auxiliary signals $\tilde{\theta}_e(t)$ and $\tilde{\theta}_r(t)$ are defined as follows

$$\tilde{\theta}_e \triangleq \hat{\theta}_e - \theta_e, \qquad \tilde{\theta}_r \triangleq \hat{\theta}_r - \theta_r \tag{26}$$

The expression in (25) can be written as follows

$$\dot{V} = e\tilde{\theta}_e - K_e e^2 + \frac{1}{\alpha_e}\tilde{\theta}_e\left(-\alpha_e e\right) - \eta\tilde{\theta}_r - K_r\eta^2 + \frac{1}{\alpha_r}\tilde{\theta}_r\left(\alpha_r\eta\right) \tag{27}$$

where the expressions in (8) and their first time derivatives were utilized. By utilizing (23), $\dot{V}(t)$ of (27) can be rewritten and upper bounded as follows

$$\dot{V} \le -\lambda_3 \|z\|^2 \tag{28}$$

where $\lambda_3 = \min\{K_e, K_r\}$. From (22), (24) and (28), it is clear that $V(z,t) \in L_\infty$; hence, $e(t), \eta(t), z(t) \in L_\infty$. From (4) and Remark 1, it is clear that $T_e(t), T_r(t) \in L_\infty$. From (7), (8), and Remark 1, it is clear that $u_e(t), u_r(t) \in L_\infty$. From (5) and the previous bounding statement, it is clear that $\dot{e}(t), \dot{\eta}(t) \in L_\infty$; hence, $\dot{T}_e(t), \dot{T}_r(t) \in L_\infty$, where (4) was utilized. From (6), and also the previous bounding statement, it is clear that $\dot{m}_r(t), \dot{m}_f(t) \in L_\infty$; thus, it is clear that $\dot{m}_c(t), H(t) \in L_\infty$. A direct application of Theorem 8.4 in (H. Khalil, 2002) can be used to prove that $z(t) \to 0$ as $t \to \infty$; thus, $e(t), \eta(t) \to 0$ as $t \to \infty$, where (23) was utilized. Based on the definition of $e(t)$ and $\eta(t)$ in (4), it is clear that if $e(t), \eta(t) \to 0$ as $t \to \infty$, then $T_e(t) \to T_{ed}(t), T_r(t) \to T_{rd}(t)$ as $t \to \infty$. Since (24) and (28) hold globally, from Theorem 8.4 in (H. Khalil, 2002), it is clear that this proof provides a global asymptotic stability (GAS) result.

APPENDIX B
Proof of Theorem 2

Lemma 1: Let the auxiliary functions $L_e(t), L_r(t) \in \Re$ be defined as follows

$$L_e \triangleq s_e\left(N_{ed} - \rho_e \operatorname{sgn}(e)\right), \qquad L_r \triangleq s_r\left(N_{rd} - \rho_r \operatorname{sgn}(\eta)\right) \tag{29}$$

where if ρ_e, ρ_r, introduced in (15) and (16) respectively, are selected to satisfy the conditions in (21), then

$$\int_{t_o}^{t} L_e(\tau) d\tau \le \zeta_{eb}, \qquad \int_{t_o}^{t} L_r(\tau) d\tau \le \zeta_{rb} \tag{30}$$

where the positive constants $\zeta_{eb}, \zeta_{rb} \in \Re$ are defined as follows

$$\zeta_{eb} \triangleq \rho_e \left|e(t_o)\right| - e(t_o) N_{ed}(t_o), \qquad \zeta_{rb} \triangleq \rho_r \left|\eta(t_o)\right| - \eta(t_o) N_{rd}(t_o). \tag{31}$$

Proof: After substituting the first expression in (9) into the first expression in (29), and then integrating, the following expression can be obtained

$$\int_{t_o}^{t} L_e(\tau) d\tau = \alpha_e \int_{t_o}^{t} e(\tau)\left[N_{ed} - \rho_e \operatorname{sgn}(e(\tau))\right] d\tau + \int_{t_o}^{t} \frac{de(\tau)}{d\tau} N_{ed} d\tau - \rho_e \int_{t_o}^{t} \frac{de(\tau)}{d\tau} \operatorname{sgn}(e(\tau)) d\tau. \tag{32}$$

After evaluating the second integral on the right-hand side of (32) by parts and evaluating the third integral, the following expression is obtained

$$\int_{t_o}^{t} L_e(\tau) d\tau = \alpha_e \int_{t_o}^{t} e(\tau)\left[N_{ed} - \rho_e \operatorname{sgn}(e(\tau))\right] d\tau - \int_{t_o}^{t} e(\tau) \frac{dN_{ed}(\tau)}{d\tau} d\tau + e(\tau) N_{ed}(\tau)\Big|_{t_o}^{t} - \rho_e \left|e(\tau)\right|\Big|_{t_o}^{t}. \tag{33}$$

The expression in (33) may be upper bounded as follows

$$\int_{t_o}^{t} L_e(\tau) d\tau = \int_{t_o}^{t} \left|e(\tau)\right| \left[\alpha_e N_{ed} + \left|\frac{dN_{ed}(\tau)}{d\tau}\right| - \alpha_e \rho_e\right] d\tau + \left|e(t)\right|\left(\left|N_{ed}(t)\right| - \rho_e\right) + \rho_e \left|e(t_o)\right| - e(t_o) N_{ed}(t_o). \tag{34}$$

From (34), it is easy to see that if is chosen according to (31), then the first inequality in (30) is hold. The second inequality in (30) can be obtained by integrating the second expression in (29) as follows

$$\int_{t_o}^{t} L_r(\tau) d\tau = \int_{t_o}^{t} \left|\eta(\tau)\right| \left[\alpha_r N_{rd} + \left|\frac{dN_{rd}(\tau)}{d\tau}\right| - \alpha_r \rho_r\right] d\tau + \left|\eta(t)\right|\left(\left|N_{rd}(t)\right| - \rho_r\right) + \rho_r \left|\eta(t_o)\right| - \eta(t_o) N_{rd}(t_o). \tag{35}$$

Proof of Theorem 2: Let the following functions $P_e(t), P_r(t) \in \Re$ be defined as follows

$$P_e \triangleq \zeta_{eb} - \int_{t_o}^{t} L_e(\tau)\, d\tau \geq 0, \qquad P_r \triangleq \zeta_{rb} - \int_{t_o}^{t} L_r(\tau)\, d\tau \geq 0 \tag{36}$$

where $L_e(t), L_r(t), \zeta_{eb}, \zeta_{rb}$ were defined in (29), and (31). The results from Lemma 1 can be used to show that $P_e(t), P_r(t)$ are non-negative functions. Let $V(y,t) \in \Re$ denote the following non-negative function

$$V \triangleq \frac{1}{2}e^2 + \frac{1}{2}C_e s_e^{\,2} + P_e + \frac{1}{2}\eta^2 + \frac{1}{2}C_r s_r^{\,2} + P_r \tag{37}$$

where $y(t) \in \Re^6$ is defined as follows

$$y \triangleq \begin{bmatrix} z & \sqrt{P_e} & \sqrt{P_r} \end{bmatrix}^T \tag{38}$$

where the composite vector $z(t) \in \Re^4$ is defined as follows

$$z \triangleq \begin{bmatrix} z_e & z_r \end{bmatrix}^T \triangleq \begin{bmatrix} e & s_e & \eta & s_r \end{bmatrix}^T \tag{39}$$

where $z_e(t) \triangleq \begin{bmatrix} e(t) & s_e(t) \end{bmatrix}$ and $z_r(t) \triangleq \begin{bmatrix} \eta(t) & s_r(t) \end{bmatrix}$. Note that (37) is bounded as follows

$$\lambda_1 \|z(t)\|^2 \leq V(y,t) \leq \lambda_2 \|z(t)\|^2 \tag{40}$$

where λ_1, λ_2 are positive constants. After taking the first time derivative of (37), the following expression can be obtained

$$\dot{V} = -\alpha_e e^2 - (K_e + \alpha_e)s_e + s_e \tilde{N}_e - \alpha_r \eta^2 - (K_r + \alpha_r)s_r + s_r \tilde{N}_r \tag{41}$$

where (9), (18), (29), and the first time derivative of (36) were utilized. To facilitate the subsequent analysis, the following inequalities can be developed from (12) through (14) (see Appendix C for further details)

$$\tilde{N}_e \leq \rho_1 \|z_e\|, \qquad \tilde{N}_r \leq \rho_2 \|z_r\| \tag{42}$$

where ρ_1, ρ_2 are positive constants,. By utilizing (42), and the triangle inequality, $\dot{V}(t)$ can be upper bounded as follows

$$\dot{V} \leq -\alpha_e |e|^2 - \alpha_r |\eta|^2 - (K_e + \alpha_e)|s_e|^2 + |s_e|\rho_1 \|z_e\| - (K_r + \alpha_r)|s_r|^2 + |s_r|\rho_2 \|z_r\|. \tag{43}$$

By utilizing (39), $\dot{V}(t)$ of (43) can be upper bounded as follows

$$\dot{V} \leq -\lambda_3 \|z\|^2 - K_e |s_e|^2 + |s_e|\rho_1 \|z_e\| - K_r |s_r|^2 + |s_r|\rho_2 \|z_r\|. \tag{44}$$

where $\lambda_3 = \min\{\alpha_e, \alpha_r\}$. After completing the squares for the last four terms on the right-hand side of (44), the following expression can be obtained

$$\dot{V} \leq -\lambda_3 \|z\|^2 + \frac{\rho_1^2}{4K_e}\|z_e\|^2 + \frac{\rho_2^2}{4K_r}\|z_r\|^2 \leq -(\lambda_3 - \lambda_4)\|z\|^2 \tag{45}$$

where $\lambda_4 = \min\left\{\frac{\rho_1^2}{4K_e}, \frac{\rho_2^2}{4K_r}\right\}$. Provided that K_e and K_r are selected so that the condition $\lambda_3 \geq \lambda_4$ is satisfied, then the following inequality can be developed

$$\dot{V} \leq W(y) \tag{46}$$

where $W(y) \in \Re$ denotes the following non-negative function

$$W(y) \leq -\gamma \|z\|^2 \tag{47}$$

where γ denotes a positive constant. From (37), (40), (46), and (47), it is clear that $V(y,t) \in L_\infty$; hence, $e(t), \eta(t), s_e(t), s_r(t), z_e(t), z_e(t), z(t), y(t) \in L_\infty$. From (4), and Remark 1, it is clear that $T_e(t), T_r(t) \in L_\infty$. From (9), it is clear that $\dot{e}(t), \dot{\eta}(t) \in L_\infty$. Thus, from Remark 1, it is clear that $\dot{T}_e(t), \dot{T}_r(t) \in L_\infty$. The previous bounding statement can be used along with (15) and (16) to prove that $u_e(t), u_r(t) \in L_\infty$. Thus, from (6), it is clear that $\dot{m}_r(t), \dot{m}_f(t) \in L_\infty$; hence, it is clear that $\dot{m}_c(t), H(t) \in L_\infty$. A direct application of Theorem 8.4 in (H. Khalil, 2002) can be used to prove that $z(t) \to 0$ as $t \to \infty$; thus, $e(t), s_e(t), \eta(t), s_r(t) \to 0$ as $t \to \infty$, where (39) was utilized. Based on the definition of $e(t)$ and $\eta(t)$ in (4), it is clear that if $e(t), \eta(t) \to 0$ as $t \to \infty$, then $T_e(t) \to T_{ed}(t), T_r(t) \to T_{rd}(t)$ as $t \to \infty$. Since (40), (46) and (47) hold globally, from Theorem 8.4 in (H. Khalil, 2002), it is clear that this proof provides a global asymptotic stability (GAS) result.

APPENDIX C
Upper Bound Development for Robust Control

By substituting (13) and (14) into (12), the expressions of $\tilde{N}_e\left(\dot{T}_e, T_e, t\right)$ and $\tilde{N}_r\left(\dot{T}_r, T_r, t\right)$ can be written as follows

$$\tilde{N}_e \equiv C_e \alpha_e \dot{e} + e, \qquad \tilde{N}_r \equiv C_r \alpha_r \dot{\eta} + \eta \tag{48}$$

which may be upper bounded as follows

$$\tilde{N}_e \leq C_e \alpha_e |\dot{e}| + |e|, \qquad \tilde{N}_r \leq C_r \alpha_r |\dot{\eta}| + |\eta|. \tag{49}$$

Using the definition of $z_e(t)$ and $z_r(t)$, given in (39), $\tilde{N}_e\left(\dot{T}_e, T_e, t\right)$, and $\tilde{N}_r\left(\dot{T}_r, T_r, t\right)$ can be bounded as follows

$$\tilde{N}_e \leq \rho_1 \|z_e\|, \qquad \tilde{N}_r \leq \rho_2 \|z_r\|. \tag{50}$$

Appendix D
NOMENCLATURE LIST

α_e	positive control gain
β_r	positive constant [Rad/sec.m^2]
C_e	engine block capacity [kJ/ºK]
C_{pc}	coolant specific heat [kJ/kg.ºK]
C_{pa}	air specific heat [kJ/kg.ºK]
C_r	radiator capacity [kJ/ºK]
e	engine temperature tracking error [ºK]
e_o	initial engine temperature tracking error [ºK]
e_{ss}	engine temperature steady state error [ºK]
ε	effectiveness of the radiator fan [%]
η	radiator temperature tracking error [ºK]
H	normalized valve position [%]
$\dot{m}_c$	pump coolant mass flow rate [kg/sec]
$\dot{m}_f$	fan air mass flow rate [kg/sec]
$\dot{m}_r$	radiator coolant mass flow rate [kg/sec]
M_1	pump coolant mass flow rate meter

M_2	radiator fan air mass flow rate meter
P_1	valve power sensor
P_2	water pump power sensor
P_3	radiator fan power sensor
P_M	cooling system power measure [W]
P_{sys}	cooling system power consumption [W]
P_v	valve power consumption [W]
ρ_e	positive constant
Q_{in}	combustion process heat energy [kW]
Q_o	radiator heat lost due to uncontrollable air flow [kW]
sgn	standard signum function
t_o	initial time [sec]
T_1	coolant temperature at engine outlet [ºK]
T_2	coolant temperature at radiator outlet [ºK]
T_3	ambient temperature sensor [ºK]
T_e	coolant temperature at the engine outlet [ºK]
T_∞	surrounding ambient temperature [ºK]
T_r	radiator outlet coolant temperature [ºK]
T_{ed}	desired engine temperature trajectory [ºK]